ARCHIVES OF CIVIL AND MECHANICAL ENGINEERING

Vol. VI 2006 No. 3

Kinematics and dynamics of some selected two-wheeled mobile robots

S. NOGA
Rzeszów University of Technology, ul. Wincentego Pola 2, 35-959 Rzeszów

In this paper, the problem of the kinematics and dynamics of two constructional conceptions of a two-wheeled mobile robot is considered. The wheeled mobile robot subjected to nonholonomic constraints moves over the inclined plane. Its trajectory consisting of the straight line and the curvilinear path described by the sinusoidal function is analyzed. The kinematic equations for arbitrarily chosen point of the system are derived by using classical equations of mechanics. Kinematic and dynamic parameters of motion from the solution of inverse kinematic and dynamic problem are obtained. Simulation results are presented to illustrate the efficiency of the approach.

Keywords: *mobile robot, nonholonomic constraints, kinematic and dynamic modelling, Lagrange's equations*

1. Introduction

The problems concerning kinematics, dynamics and control of wheeled mobile robots gain more and more attention. This results mainly from the fact that wheeled mobile robots are very often used in industry, especially where the contribution of an operator to some technological processes is not recommended. The mobile robot under investigation is a system which rolls on conventional wheels and is subjected to nonholonomic constrains. Fundamental theory of nonholonomic systems is developed in a number of monographs by, for example, Gutowski [1], Nejmark and Fufajev [2]. The kinematic modelling of mobile robots is investigated by many researchers. The problem of the kinematics of a two-wheeled mobile robot is analyzed in [3–6, 8–10]. In [6, 8, 9], a natural orthogonal complement is applied to a wheeled mobile robot. The problem of motion of the mobile robot along the curvilinear trajectory is discussed in the paper [10], excluding the kinematics of bracket and caster wheel. In papers [3, 4], the kinematics of this system using classical equations of mechanics is described, including the kinematics of bracket and caster wheel. The problem of the dynamics of a mobile robot is considered in papers [4, 6, 8, 11]. In papers [6, 8], a natural orthogonal complement is applied to a wheeled mobile robot. The problem of neural modelling of the mobile robot is discussed in paper [11], excluding the dynamics of a bracket and a caster wheel. In paper [4], the dynamics of this system using classical equations of mechanics is described. This paper continues the recent author's investigations concerning the kinematics and dynamics of mobile robots [3–5, 10, 11].

The present paper is organized as follows. Section two describes the mobile robot system under study. In sections three and four, the kinematics of a two-wheeled mobile robot is studied. In section five, the dynamics of the mobile robot is analyzed. Section six presents some simulation results, and section seven gives some concluding remarks.

2. Model of the system

An assumed model of the mobile robot is presented in Figure 1. The basic units of the model are as follows: frame 4, driving and steering wheels 1 and 2, and bracket with caster wheel 3. Wheels 1 and 2, mounted on the shafts, are driven separately by two electric motors. Wheels rotate about their axes, whose positions are invariable in relation to the frame. The third wheel is mounted on a rotary bracket. In the modelling of the mobile robot system, the following assumptions are adopted:

- There is no slipping between the wheel and the floor, i.e., rolling contact is maintained.
- The vehicle cannot move sideways to maintain the nonholonomic constraint.
- The motion of the mobile robot is confined to the plane *xy*.

Paper [7] presents the specifications and controls of the mobile robot shown below.

The coordinates α_1, α_2, and α_3 are the angles of rotation of wheels 1, 2, and 3, respectively. The angle of rotation of the formative wheel 1z is denoted by α. The angle β is the angle of instantaneous angular displacement of frame 4.

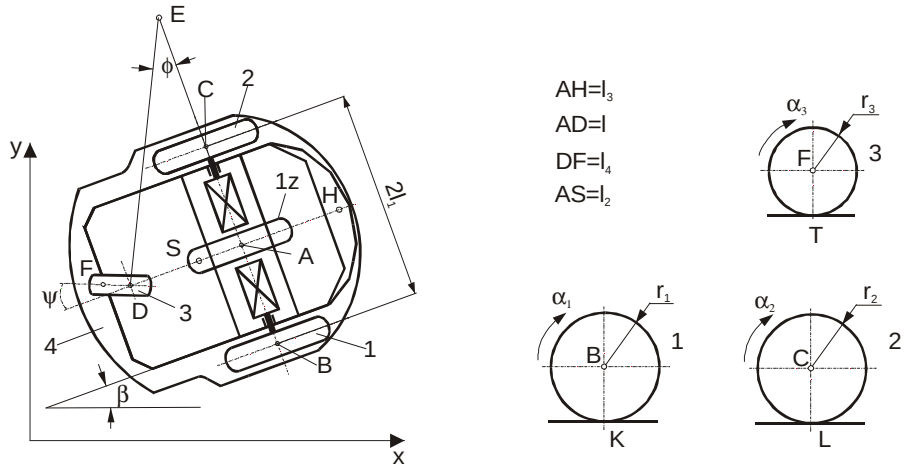

Fig. 1. The two-wheeled mobile robot

The angle ψ is the angle between the longitudinal symmetry axis of the chassis and the bracket. The following elements: l, l_1, l_2, l_3, l_4 are the lengths, and r_1, r_2,

r_3 are the radii defined in Figure 1. The radius r is the radius of the formative wheel 1z . The point *A* is a characteristic point of the frame and the point of intersection of the frame longitudinal symmetry axis with the axis of rotation of wheels 1 and 2. The points *B*, *C*, and *F* are the centres of masses of wheels 1, 2, and 3, respectively. The point *S* is the centre of mass of chassis 4. The point *D* is the connection point of bracket 3 and frame 4.

The position and orientation of the mobile robot are described by seven coordinates: x_A, y_A – the Cartesian coordinates of the point *A*; α_1, α_2, α_3, β, ψ – the angle coordinates.

The mobile robot constitutes a nonholonomic planar system. If no slipping and no sideway motions are assumed, the mobile robot has two degrees of freedom only. One can choose the angles of driving wheels as generalized coordinates for the convenience of control design. The objective of the kinematic analysis of the mobile robot is to derive the kinematic parameters of the system in terms of generalized coordinates.

In the present paper, two conceptions of the constructional schemes of this kind of robot are analyzed. When the centre *S* of mass is situated behind the axis of wheels 1 and 2 (see Figure 2a), we deal with the so-called dragging system [4]. When the point *S* is situated before the axis of wheels 1 and 2 (see Figure 2b), we deal with the so-called propelling system [4].

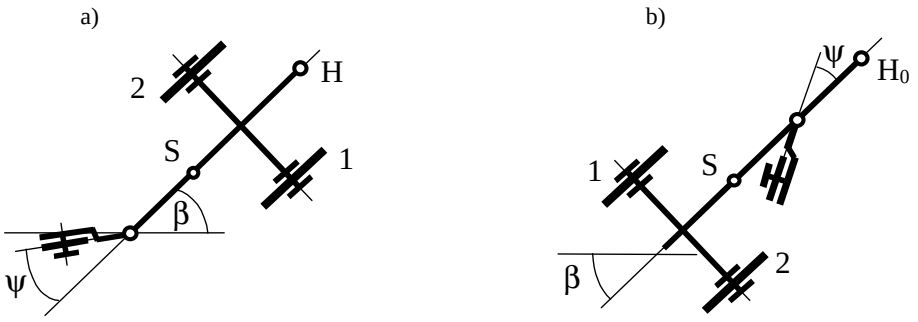

Fig. 2. Schematic diagrams of the two-wheeled mobile robot

3. Kinematics of the dragging system

The robot under consideration is moved on the plane. The chassis and the bracket with the caster wheel undergo planar motion. The velocity distribution of characteristic points of the system is displayed in Figure 3.

The point *E* is an instantaneous centre of chassis 4, and the point *G* is the instantaneous centre of the bracket.

According to the nonholonomic constraints and nonslipping condition, the robot has to move in the direction of the symmetry axis, i.e.:

$$\dot{x}_A = v_A \cos\beta, \qquad \dot{y}_A = v_A \sin\beta, \tag{1}$$

where v_A is the velocity of the point *A*. Likewise, the bracket has to move in the direction of the symmetry axis, i.e.:

$$\dot{x}_F = v_F \cos(\beta - \psi), \qquad \dot{y}_F = v_F \sin(\beta - \psi), \tag{2}$$

where v_F is the velocity of the point *F* (see Figures 1 and 3), and (x_F, y_F) are the coordinates of the point *F* given directly by:

$$x_F = x_A - l\cos\beta - l_4 \cos(\beta - \psi), \qquad y_F = y_A - l\sin\beta - l_4 \sin(\beta - \psi). \tag{3}$$

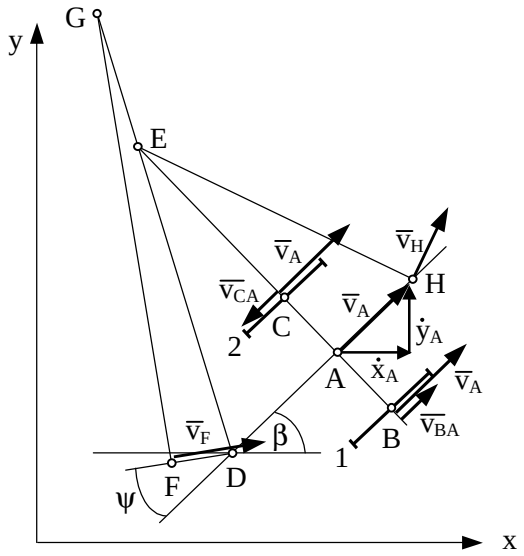

Fig. 3. The velocity distribution of the system

From Equations (1) – (3), the angular velocity of the bracket with respect to the chassis is determined [4]:

$$\dot{\psi} = \frac{1}{l_4}\left[\dot{\beta}\left(l\cos\psi + l_4\right) - v_A \sin\psi\right]. \tag{4}$$

Taking into account kinematic equations for the points *B*, *C*, and *F*, the angular velocities of wheels 1, 2, and 3 are given by [4]:

$$\dot{\alpha}_1 = \frac{v_A}{r} + \dot{\beta}\frac{l_1}{r}, \qquad \dot{\alpha}_2 = \frac{v_A}{r} - \dot{\beta}\frac{l_1}{r}, \qquad \dot{\alpha}_3 = \frac{v_A}{r_3}\cos\psi + \dot{\beta}\frac{l}{r_3}\sin\psi. \tag{5}$$

Taking into account the velocity distribution for the points *A*, *B*, and *C* (Figure 3) and Equation (5), the angular velocity of formative wheel 1z is expressed by:

$$\alpha = \frac{1}{2}(\alpha_1 + \alpha_2). \tag{6}$$

4. Kinematics of the propelling system

The other system is the so-called propelling system. Likewise, the chassis and the bracket with the caster wheel undergo planar motion. The velocity distribution of the characteristic points of the system is shown in Figure 4.

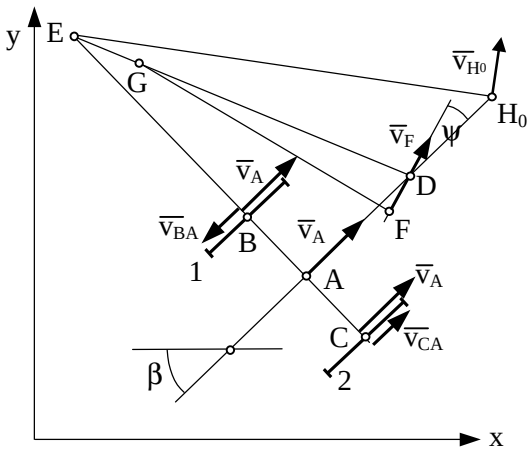

Fig. 4. The velocity distribution of the system

The corresponding formulae describing the kinematics of propelling system are as follows [4]:

$$\dot{x}_F = v_F\cos(\beta + \psi), \qquad \dot{y}_F = v_F\sin(\beta + \psi), \tag{7}$$

$$x_F = x_A + l\cos\beta - l_4\cos(\beta + \psi), \qquad y_F = y_A + l\sin\beta - l_4\sin(\beta + \psi), \tag{8}$$

$$\dot{\psi} = \frac{1}{l_4}\left[\dot{\beta}(l\cos\psi - l_4) - v_A\sin\psi\right], \tag{9}$$

$$\dot{\alpha}_1 = \frac{v_A}{r} - \dot{\beta}\frac{l_1}{r}, \qquad \dot{\alpha}_2 = \frac{v_A}{r} + \dot{\beta}\frac{l_1}{r}, \qquad \dot{\alpha}_3 = \frac{v_A}{r_3}\cos\psi + \dot{\beta}\frac{l}{r_3}\sin\psi. \tag{10}$$

5. Dynamics of the mobile robot

In this section, the dynamics of constructional schemes is described based on classical equations of mechanics; the dynamics of the bracket and the caster wheel is excluded. The motion of the robot is considered in the plane xy inclined to the horizontal plane x_0y_0, where γ is the angle of inclination of the motion plane (Figure 5).

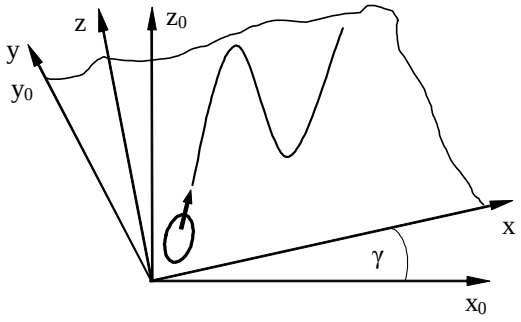

Fig. 5. The motion plane of the system

The mathematical model of the mobile robot described by n generalized coordinates grouped together in the vector q and subjected to $s < n$ nonholonomic constraints is derived. The formulation of the model of interest is based on Lagrange's equations for constrained mechanical systems.

Lagrange's equations of the system at hand have the form [1, 2, 6]:

$$\frac{d}{dt}\left(\frac{\partial E}{\partial \dot{q}}\right) - \frac{\partial E}{\partial q} + \frac{\partial V}{\partial q} = Q + J^T(q)\lambda, \tag{11}$$

where $E = E(q, \dot{q})$ is the kinetic energy of the system, V is the Newtonian potential of the system, Q is the vector of generalized forces, $J(q)$ is the matrix associated with the constraints, q is the vector of generalized coordinates, $\dot{q}$ is the vector of generalized velocities, λ is the vector of the Lagrange multipliers, and the superscript T is the transpose of a matrix operator.

The matrix $J(q)$ is obtained from the equations of kinematic constraints in terms of generalized velocities, i.e., [1, 2, 6]:

$$J(q)\,\dot{q} = 0. \tag{12}$$

5.1. Dynamics of the dragging system

The position and orientation of the mobile robot excluding the bracket with the caster wheel are described by the following vector of generalized coordinates:

$$q = [x_A, y_A, \beta, \alpha]^T. \tag{13}$$

As is mentioned earlier, the mobile robot has two degrees of freedom only. There are two nonholonomic constraints. From Equation (12) the matrix $J(q)$ is given by:

$$J(q) = \begin{bmatrix} 1 & 0 & 0 & -r\cos\beta \\ 0 & 1 & 0 & -r\sin\beta \end{bmatrix}, \tag{14}$$

where $r = r_1 = r_2$.

It is shown that the kinetic energy of the dragging system takes the form [3, 5]:

$$\begin{aligned} E = {} & \frac{1}{2}(m_1 + m_2 + m_4)\dot{x}_A^2 + \frac{1}{2}(m_1 + m_2 + m_4)\dot{y}_A^2 + (m_1 - m_2)l_1\dot{\beta}(\dot{x}_A\cos\beta \\ & + \dot{y}_A\sin\beta) + m_4 l_2\dot{\beta}(\dot{x}_A\sin\beta - \dot{y}_A\cos\beta) + (I_{z1} - I_{z2})h_1\dot{\alpha}\,\dot{\beta} + \frac{1}{2}(I_{z1} + I_{z2})h_1^2\dot{\beta}^2 \\ & + \frac{1}{2}\left(m_1 l_1^2 + m_2 l_1^2 + m_4 l_2^2 + I_{x1} + I_{x2} + I_{z4}\right)\dot{\beta}^2 + \frac{1}{2}(I_{z1} + I_{z2})\dot{\alpha}^2, \end{aligned} \tag{15}$$

where m_1, m_2, m_4 are the masses of members of the system, I_{x1}, I_{x2}, I_{z1}, I_{z2}, I_{z4} are the inertia moments of movable members of the system, $h_1 = l_1/r$ is a nondimensional parameter.

Gravitation potential of the dragging system is:

$$V = (m_1 + m_2 + m_4)\, g \sin\gamma\, x_A - m_4 g\, l_2 \sin\gamma\cos\beta + \left[(m_1 + m_2)r + m_4 h_S\right] g\cos\gamma, \tag{16}$$

where h_S is the distance between the centre of inertia and the motion plane of the robot, g is the acceleration due to gravity.

The vector of unconstrained generalized forces is given by:

$$\tau = \begin{bmatrix} 0 \\ 0 \\ (M_1 - M_2 - N_1 f_1 + N_2 f_2)h_1 \\ M_1 + M_2 - N_1 f_1 - N_2 f_2 \end{bmatrix}, \tag{17}$$

where M_1, M_2 are the driving torques, N_1, N_2 are the axial forces acting on the wheels, f_1, f_2 are the coefficients of rolling friction.

When the robot motion over the inclined plane is realized, the value of the resisting force depends on the robot orientation on the motion plane *xy*. The axial forces are expressed by [4]:

$$\begin{aligned} N_1 &= N_0\left[\left(1-\frac{l_2}{l}\right)\cos\gamma - h_S\sin\gamma\left(\frac{1}{l_1}\sin\beta+\frac{1}{l}\cos\beta\right)\right], \\ N_2 &= N_0\left[\left(1-\frac{l_2}{l}\right)\cos\gamma + h_S\sin\gamma\left(\frac{1}{l_1}\sin\beta-\frac{1}{l}\cos\beta\right)\right], \end{aligned} \tag{18}$$

where $N_0 = 0.5(m_1+m_2+m_4)g$.

Taking into account Equations (14)–(17), Lagrange's equations (11) for this model are as follows:

$$\begin{aligned} &m_4 l_2\ddot{\beta}\sin\beta + (2m_1+m_4)r\ddot{\alpha}\cos\beta + m_4 l_2\dot{\beta}^2\cos\beta - (2m_1+m_4)r\dot{\alpha}\dot{\beta}\sin\beta \\ &\qquad + (m_1+m_2+m_4)g\sin\gamma = \lambda_1, \\ &-m_4 l_2\ddot{\beta}\cos\beta + (2m_1+m_4)r\ddot{\alpha}\sin\beta + m_4 l_2\dot{\beta}^2\sin\beta + (2m_1+m_4)r\dot{\alpha}\dot{\beta}\cos\beta = \lambda_2, \\ &(2m_1 l_1^2 + m_4 l_2^2 + 2I_{x1} + 2I_{z1}h_1^2 + I_{z4})\ddot{\beta} - m_4 l_2 r\dot{\alpha}\dot{\beta} + m_4 g\, l_2\sin\gamma\sin\beta \\ &\qquad = (M_1 - M_2 - N_1 f_1 + N_2 f)h_1, \\ &(2m_1 + m_4 + \frac{2}{r^2}I_{z1})r^2\ddot{\alpha} + m_4 l_2 r\dot{\beta}^2 + (m_1+m_2+m_4)g\, r\sin\gamma\cos\beta \\ &\qquad = M_1 + M_2 - N_1 f_1 - N_2 f_2, \end{aligned} \tag{19}$$

where λ_1, λ_2 are the Lagrange multipliers.

5.2. Dynamics of the propelling system

Likewise, the position and orientation of the mobile robot are described by the vector of generalized coordinates:

$$q = [x_A, y_A, \beta, \alpha]^T. \tag{20}$$

The kinetic energy of the propelling system takes the form:

$$E=\frac{1}{2}(m_1+m_2+m_4)\,\dot{x}_A^2+\frac{1}{2}(m_1+m_2+m_4)\,\dot{y}_A^2+m_4 l_2\dot{\beta}(-\dot{x}_A\sin\beta+\dot{y}_A\cos\beta)$$
$$+\frac{1}{2}(I_{z1}+I_{z2})\,h_1^2\dot{\beta}^2+\frac{1}{2}(m_1 l_1^2+m_2 l_1^2+m_4 l_2^2+I_{x1}+I_{x2}+I_{z4})\,\dot{\beta}^2+\frac{1}{2}(I_{z1}+I_{z2})\,\dot{\alpha}^2. \quad (21)$$

Gravitation potential for this system is expressed by:

$$V=(m_1+m_2+m_4)\,g\sin\gamma\,x_A+m_4 g\,l_2\sin\gamma\cos\beta+[(m_1+m_2)\,r+m_4 h_S]\,g\cos\gamma. \quad (22)$$

The vector of unconstrained generalized forces is given by:

$$\tau=\begin{bmatrix}0\\0\\(-M_1+M_2+N_1 f_1-N_2 f_2)h_1\\M_1+M_2-N_1 f_1-N_2 f_2\end{bmatrix}, \quad (23)$$

where the resisting forces are:

$$N_1=N_0\left[\left(1-\frac{l_2}{l}\right)\cos\gamma+h_S\sin\gamma\left(\frac{1}{l_1}\sin\beta+\frac{1}{l}\cos\beta\right)\right],$$
$$N_2=N_0\left[\left(1-\frac{l_2}{l}\right)\cos\gamma-h_S\sin\gamma\left(\frac{1}{l_1}\sin\beta-\frac{1}{l}\cos\beta\right)\right]. \quad (24)$$

Lagrange's equations (11) for this case are written in the form:

$$\begin{aligned}
&-m_4 l_2\ddot{\beta}\sin\beta+(2m_1+m_4)\,r\ddot{\alpha}\cos\beta-m_4 l_2\,\dot{\beta}^2\cos\beta-(2m_1+m_4)\,r\dot{\alpha}\,\dot{\beta}\sin\beta\\
&\qquad+(m_1+m_2+m_4)\,g\sin\gamma=\lambda_1,\\
&m_4 l_2\ddot{\beta}\cos\beta+(2m_1+m_4)\,r\ddot{\alpha}\sin\beta-m_4 l_2\,\dot{\beta}^2\sin\beta+(2m_1+m_4)\,r\dot{\alpha}\dot{\beta}\cos\beta=\lambda_2,\\
&(2m_1 l_1^2+m_4 l_2^2+2I_{x1}+2I_{z1}h_1^2+I_{z4})\,\ddot{\beta}+m_4 l_2 r\dot{\alpha}\dot{\beta}-m_4 g\,l_2\sin\gamma\sin\beta\\
&\qquad=(-M_1+M_2+N_1 f_1-N_2 f_2)h_1,\\
&\left(2m_1+m_4+\frac{2}{r^2}I_{z1}\right)r^2\ddot{\alpha}-m_4 l_2 r\,\dot{\beta}^2+(m_1+m_2+m_4)\,g\,r\sin\gamma\cos\beta\\
&\qquad=M_1+M_2-N_1 f_1-N_2 f_2.
\end{aligned} \quad (25)$$

6. Simulation

In this section, simulation results of inverse kinematic and dynamic problem using the systems suggested earlier are presented. Computer simulation makes it possible to find the solution for the system of Equations (4), (5), (9), (10), (19) and (25), and then to determine the kinematic and dynamic parameters of motion being of our interest. In the first step, the problem of inverse kinematics is realized. Considering the problem of inverse dynamics, we obtain the required time histories of motion parameters as a result of solving inverse kinematics problem. The scheme of executed process is shown in Figure 6.

Fig. 6. The scheme of the problem of inverse dynamics

It is assumed that the point H (the dragging system) or the point H_0 (the propelling system) moves along the trajectory that consists of straight lines and sinusoidal path of the amplitude $A_0 = 1$ [m] and the period $L = 2.45$ [m] described by the following function:

$$y_H = A_0 \sin \omega x_H , \tag{26}$$

where $\omega = 2\pi/L$.

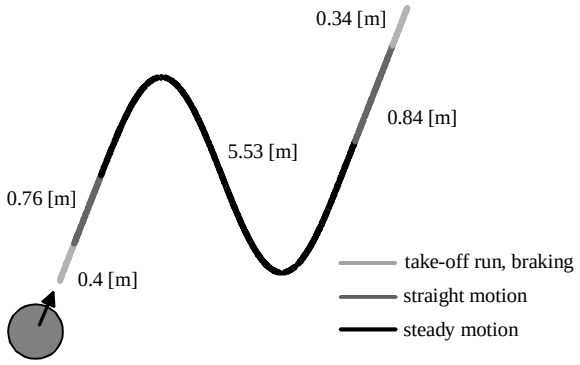

Fig. 7. The assigned trajectory of characteristic point H (H_0) of the system

The motion phases, i.e.: take-off run, steady motion and braking, are analyzed. The parameters characterizing the mobile robot used in calculations are shown in the Table.

Table. Parameters characterizing the two-wheeled mobile robot

m_1 [kg]	m_4 [kg]	I_{x1} [kg·m²]	I_{z1} [kg·m²]	I_{z4} [kg·m²]	N_0 [N]
1.5	5.67	0.00255	0.0051	0.154	43.35
f_1 [m]	l [m]	l_1 [m]	l_2 [m]	l_3 [m]	l_4 [m]
0.01	0.217	0.163	0.07	0.133	0.025
l_5 [m]	r [m]	r_3 [m]	h_S [m]		
0.27	0.0825	0.035	0.1		

In this table, $l_5 = AH$. It is assumed that $f_1 = f_2$ and $m_1 = m_2$. The velocity v_A of the point A equal to 0.3 m/s is used in the calculations and is assumed to be constant. Parameters of the trajectory are selected experimentally.

6.1. Inverse kinematic problem

In this subsection, the results of the inverse kinematic problem of both systems considered are presented. For all examples the time histories of the parameters of motion, including angular velocities and angles of rotation of wheels 1, 2, and 3 and angular velocity and angle of rotation of chassis 4 as well as angular velocity and angle of rotation of the bracket with respect to the chassis, are obtained by using a computer simulation.

Parameters of motion of the dragging system are displayed in Figures 8 and 9. Substantial changes in the angular velocities when the robot is on the move along the turn (upper and lower vertices of the sinusoidal trajectory) are observed. When the robot over the straight line is moved, the angular velocities $\dot{\beta}$ and $\dot{\psi}$ equalize and are equal to null. The angles β and ψ are changed when the system is on the move along the turn.

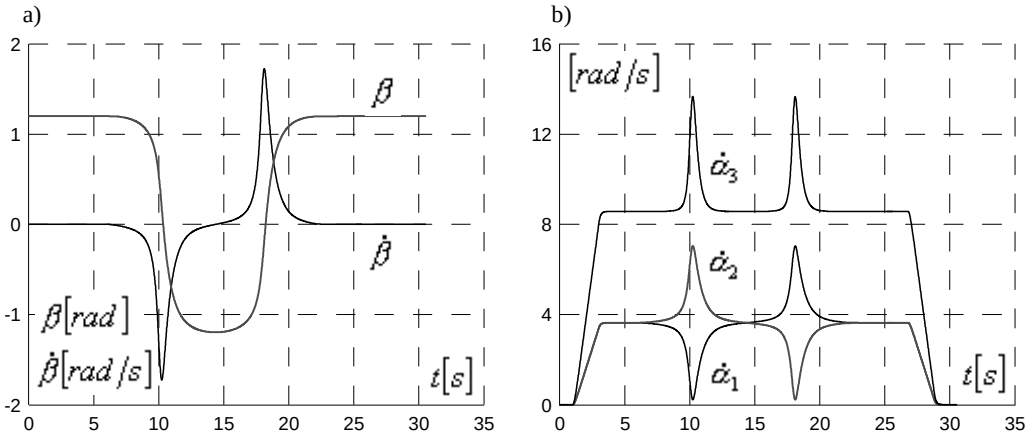

Fig. 8. Time histories of motion parameters of the dragging system

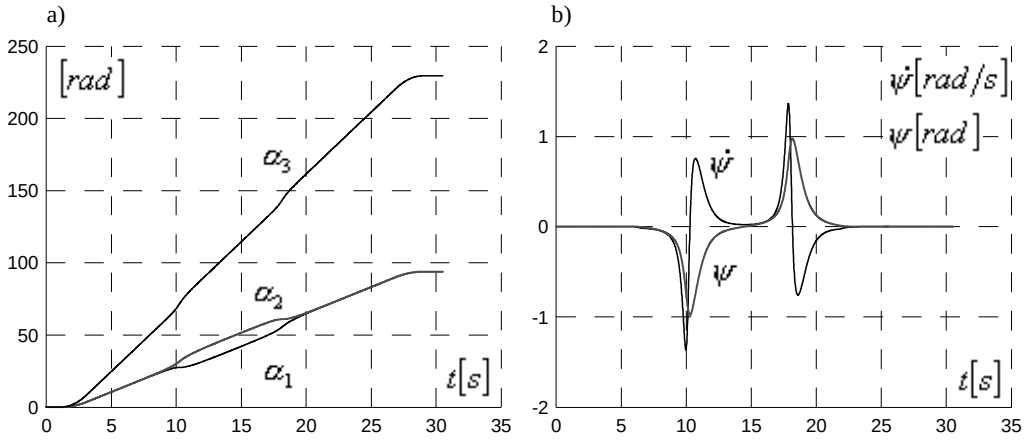

Fig. 9. Time histories of motion parameters of the dragging system

In Figures 10 and 11, the parameters of motion of the propelling system are shown.

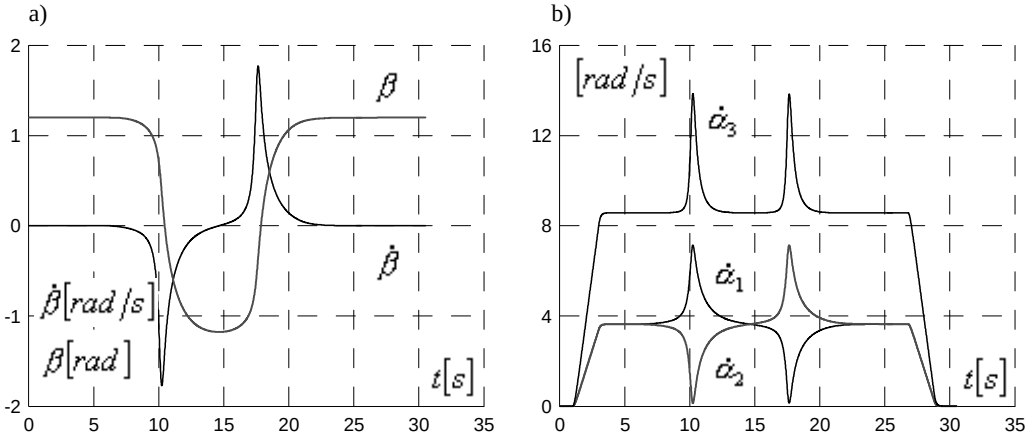

Fig. 10. Time histories of motion parameters of the propelling system

Likewise, the substantial changes of kinematic parameters when the robot is on the move along the turn are observed. Computer simulation results show that the slight qualitative and quantitative differences between the dragging and propelling systems appear. The parameters of motion are needed to solve the problem of the inverse dynamics, i.e., to find the driving torques of wheels 1 and 2, respectively.

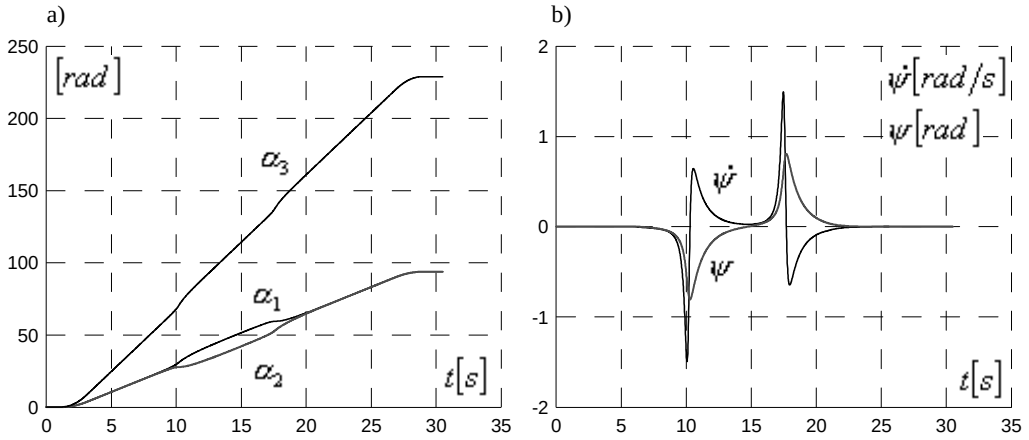

Fig. 11. Time histories of motion parameters of the propelling system

6.2. Inverse dynamic problem

In this subsection, simulation results of an inverse dynamic problem are presented. Computer simulation makes it possible to find the solution for a system of Equations (19) and (25), i.e., to determine the driving torques and the Lagrange multipliers. For both systems the cases where $\gamma = \pi/24$ and $\gamma = 0$ are solved.

Parameters of motion of the dragging model are displayed in Figures 12 and 13.

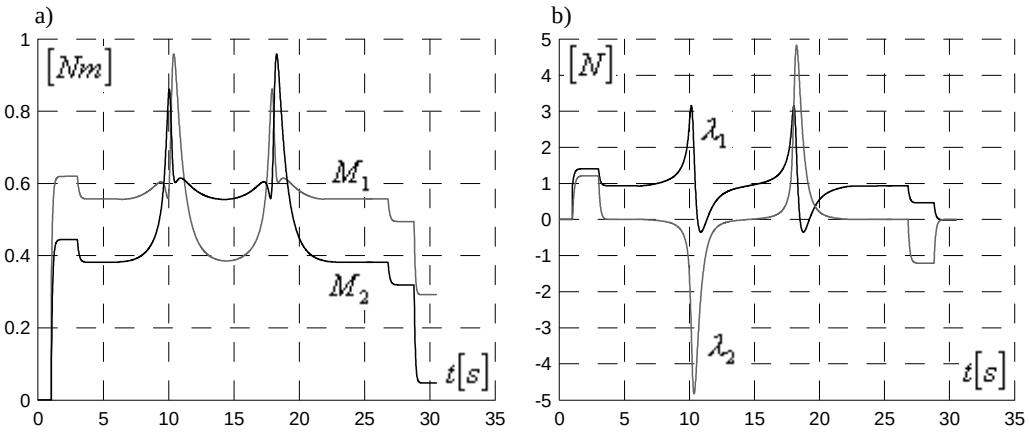

Fig. 12. Time histories of the driving torques (a) and the Lagrange multipliers (b), ($\gamma = \pi/24$)

Substantial changes of the driving torques and the Lagrange multipliers when the robot is on the move along the turn are observed.

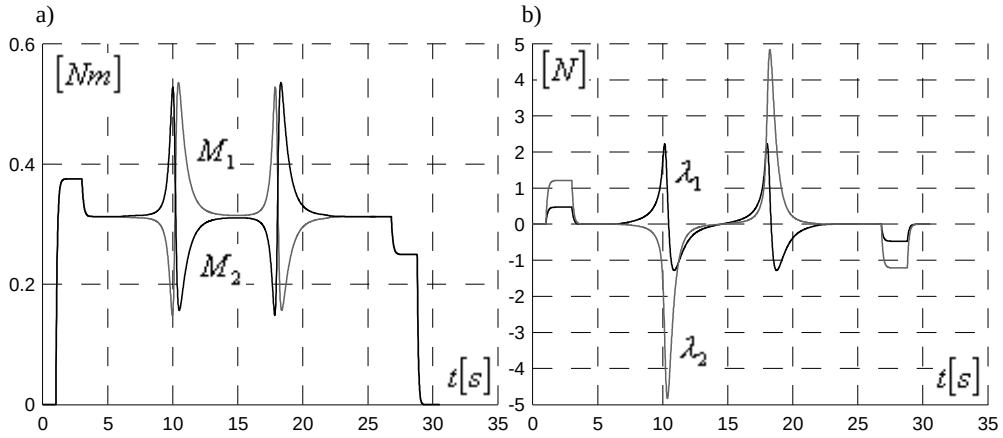

Fig. 13. Time histories of the driving torques (a) and the Lagrange multipliers (b), ($\gamma = 0$)

Considerable changes in the driving torques and the Lagrange multipliers at the take-off run time and braking and when the robot is on the move along the turn are shown in Figures 12 and 13.

The parameters of motion of the propelling model are displayed in Figures 14 and 15.

Likewise, considerable changes in the driving torques and the Lagrange multipliers at the take-off run time and braking and when the robot is on the move along the turn are observed.

For both cases of the systems analyzed, extremum values of the driving torques and the Lagrange multipliers are higher for the propelling system compared to the dragging system.

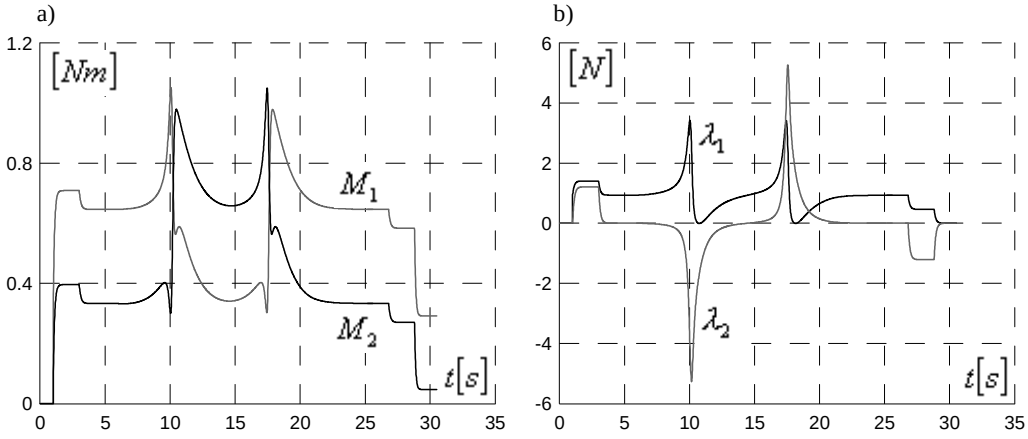

Fig. 14. Time histories of the driving torques (a) and the Lagrange multipliers (b), ($\gamma = \pi/24$)

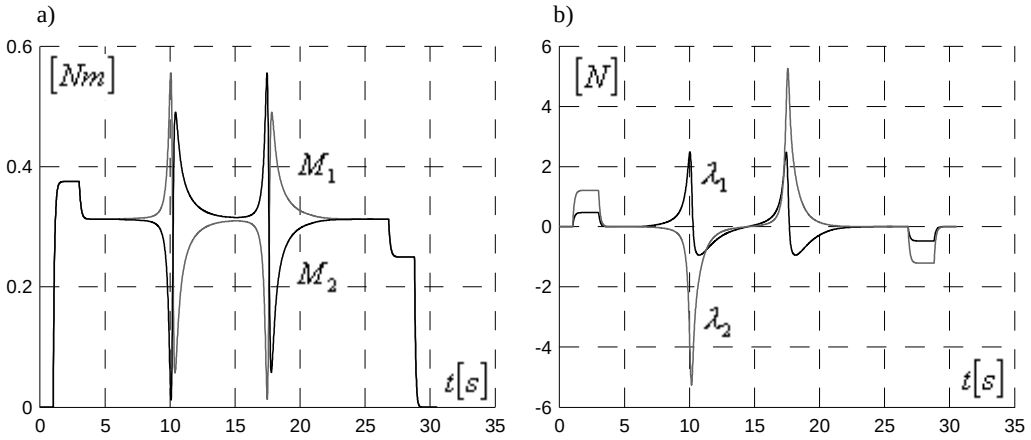

Fig. 15. Time histories of the driving torques (a) and the Lagrange multipliers (b), ($\gamma = 0$)

7. Conclusions

Kinematic and dynamic analysis of the system is involved in the problems of inverse kinematics and dynamics. Motions of the dragging and propelling systems using classical equations of mechanics are described including the kinematics of the bracket and the caster wheel.

In the present paper, the curvilinear trajectory of the point H (the dragging system) or the point H_0 (the propelling system) of the two-wheeled mobile robot is considered. The trajectory planing is an important problem in the process of identification in real time. Such a trajectory should have a persistence of excitation (PE) condition of the above mentioned mobile robot. On the other hand, the trajectory needed should be realized by the robot.

Based on classical equation of mechanics the dynamics of the systems analyzed is described, including the motion over the inclined plane subjected to nonholonomic constraints.

In an available literature, the author has not found examples of using this method for the analysis of the problems of inverse kinematics and dynamics of a two-wheeled mobile robot that includes a bracket and a caster wheel and moves over the inclined plane.

Time histories of motion parameters can be utilized to plan the movement trajectory system in joint variables or to solve the problem of the control of this object.

Simulation results show that the slight qualitative and quantitative differences (with the exception of the motion over the inclined plane) between the dragging and propelling systems emerge.

This consideration can be applied to kinematic and dynamic description of any wheeled mobile robot model, independently of the number of its wheels.

Acknowledgement

The author would like to thank the reviewers for their careful reading of the paper and their helpful comments.

References

[1] Gutowski R.: *Analytical Mechanics*, PWN, Warsaw, 1971 (in Polish).
[2] Nejmark J.I., Fufajev N.A.: *Dynamics of Nonholonomic Systems*, PWN, Warsaw, 1971 (in Polish).
[3] Noga S.: *Kinematics of an optional nonholonomic mobile robot*, Proceedings of the 3th Ukrainian–Polish Scientific Conference *Mechanics and Informatics*, Khmelnitskij, 2005, pp. 77–80.
[4] Noga S.: *Kinetics of a two wheeled mobile robot*, PhD Thesis, Faculty of Mechanical Engineering and Aeronautics, Rzeszów University of Technology, Rzeszów, 2004 (in Polish).
[5] Noga S.: *Modelling and dynamical analysis of the two wheeled mobile robot*, Technical Journal, Cracow University of Technology Publishers, Cracow, 2005, z. 14–M, pp. 63–81 (in Polish).
[6] Ostrovskaya S., Angeles J.: *Nonholonomic systems revisited within the framework of analytical mechanics*, Applied Mechanics Reviews, 1998, Vol. 51, No. 7, pp. 415–433.
[7] *Pioneer 2 Mobile Robot – Operations Manual*, 1999, ActivMEDIA ROBOTICS, LLC.
[8] Yu Q., Chen I.-M.: *A general approach to the dynamics of nonholonomic mobile manipulator systems*, Journal of Dynamic Systems, Measurement and Control, 2002, Vol. 124, pp. 512–521.
[9] Zhang Y.L., Velinsky S.A., Feng X.: *On the tracking control of differentially steered wheeled mobile robots*, Journal of Dynamic Systems, Measurement and Control, 1997, Vol. 119, pp. 455–461.
[10] Żylski W., Hendzel Z., Noga S.: *Inverse kinematics problem of a mobile 2-wheeled robot*, Proceedings of the International Scientific Conference *Mechanics 2000*, Rzeszów, 2000, pp. 491– 495.
[11] Żylski W., Noga S.: *Neural modelling dynamics of a mobile wheeled robot*, Proceedings of the 11th International Symposium on Dynamics of Structures, Rzeszów–Arłamów, 2002, pp. 629–636 (in Polish).

Kinematyka i dynamika wybranych mobilnych robotów dwukołowych

Opisano modelowanie wybranych rozwiązań konstrukcyjnych mobilnego robota dwukołowego oznaczonych jako układ ciągniony oraz układ napędzany. Rozważany pojazd jest układem z więzami nieholonomicznymi. Analizowane są przypadki, w których roboty poruszają się po powierzchni nachylonej. Dla przyjętych modeli koncepcyjnych rozwiązano zadanie odwrotne kinematyki i dynamiki, zakładając, że wybrane punkty pojazdów poruszają się po torze złożonym z odcinków linii prostych i łuku w kształcie funkcji sinus. Zaprezentowano zależności wybranych parametrów kinematycznych i dynamicznych układów od czasu, które otrzymano w wyniku numerycznego rozwiązania wyprowadzonych wcześniej równań ruchu.

Z przedstawionych wyników i metodyki postępowania mogą korzystać potencjalni konstruktorzy na etapie rozważań koncepcyjnych w procesie projektowania tego typu pojazdów.